Final Draft
of the original manuscript:

Wittenberg, E.; Abetz, V.:

New post modification route for styrene butadiene copolymers leading to supramolecular hydrogen bonded networks – Synthesis and thermodynamic analysis of complexation

In: Polymer (2017) Elsevier

DOI: 10.1016/j.polymer.2017.06.001

New post modification route for styrene butadiene copolymers leading to supramolecular hydrogen bonded networks - Synthesis and thermodynamic analysis of complexation

Elisabeth Wittenberg[a], Volker Abetz [a, b,*]

[a] Institute of Physical Chemistry, University of Hamburg, Martin-Luther-King-Platz 6, 20146 Hamburg, Germany

[b] Institute of Polymer Research, Helmholtz-Zentrum Geesthacht, Max-Planck-Str. 1, 21502 Geesthacht, Germany

E-mail: volker.abetz@hzg.de

Graphical Abstract (TOC)

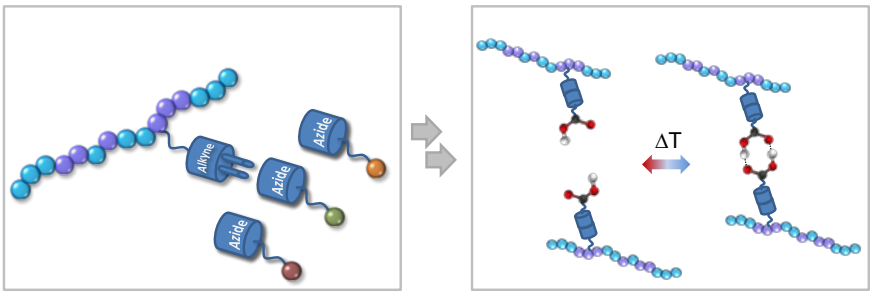

Abstract

In this work we present a new and simple post modification route for styrene-butadiene copolymers using well established reactions including hydrochlorination and Steglich esterification to obtain alkyne functionalized styrene-butadiene copolymers. The alkyne linker allows the introduction of arbitrary azides into the styrene-butadiene copolymers via copper catalyzed azide alkyne cycloaddition and this leads to a toolbox of diverse functional polymers. This method gives new opportunities regarding modification strategies and is used in this work to obtain supramolecular styrene-butadiene copolymer networks by introduction of a benzoic acid derivative. This simple supramolecular motif forms temperature dependent hydrogen bonding complexes which can be quantitatively studied by FTIR spectroscopy. We found that the equilibrium constant, ΔH and ΔS are changing with temperature which can be attributed to a structural modification: the dissociation.

Keywords: Post modification, supramolecular polymers, hydrogen bonding, IR-spectroscopy, complex formation.

Highlights

- A new and simple post modification route for styrene-butadiene copolymers is presented.
- The presented reaction pathway leads to a toolbox of diverse functional polymers.
- The equilibrium constant, ΔH and ΔS of complex formation are temperature dependent.

1. Introduction

In the last decades supramolecular chemistry has become a continuously growing field in polymer science. In contrast to conventional polymers, supramolecular polymers and networks are formed by non-covalent interactions such as π-π [1], metal-ligand [2] and hydrogen bonding [3] between small molecules or telechelics. The primary feature of such polymers is the spontaneous assembly of the precursor building blocks to form larger structures [4, 5]. This is well-known from telechelic networks [6, 7]. The precursor building blocks (telechelic units) are end-functionalized with e.g. hydrogen bonding motifs and can form longer chains and networks by self-assembly [8]. This was reported by Meijer and Palmans et al [9]. Another possibility is the modification of the polymer not only at the polymer chain ends, but also along the polymer main chain by introduction of hydrogen bonding motifs which offers the possibility to tune the properties of the polymer to a great extent [10]. Three particular parameters affect the properties of these polymers: 1) the nature of the hydrogen bond, 2) the degree of modification and therefore the number of units bound together and 3) the molecular mobility of the polymer chains [11, 12]. The hydrogen bonding motifs may be entropically hindered to form complexes due to the polymer chains on which they are bound [13]. The properties of the polymer can of course not only be tailored by post modification, but also by designing the polymer itself. For example, combining polymer blocks with different chemical or physical properties, results in tailor-made block copolymers which can be designed for their application. The copolymers of styrene and butadiene are popular thermoplastic elastomers (TPE) which combine the properties of thermoplastic polystyrene and elastomeric polybutadiene. From a post modification point of view the butadiene units of these copolymers contain highly reactive double bonds while the polystyrene parts are chemically fairly inactive [14-16]. Modified styrene-butadiene copolymers are used to produce electrospun fibers [17, 18], nanocomposites [19, 20] and the probably largest field of application is the usage of modified styrene-butadiene copolymers as additives for bitumen [21] so far.

The modification of double bonds is essential in organic chemistry and well-studied since years. Electrophilic [22], nucleophilic [23] as well as radical addition [24, 25] reactions are often used for this purpose. Due to the lower reactivity of the double bonds in polymers in contrast to molecules with low molecular weight, the number of potential reactions is significantly reduced. Peng et al. [15] reported a modification route for polybutadienes by epoxidation, hydrolysis and following carbamate ester

forming using sulfonyl isocyanates. This procedure is a good alternative to the addition of 4-substituted 1,2,4-triazoline-3,5-diones to polydienes, which is one of the most effective methods for modifying polydienes quantitatively [26-30]. Dienophiles like 4-substituted 1,2,4-triazoline-3,5-diones are highly reactive and can instantaneously be added to olefins via an ene-reaction. But the main issue is the synthesis of the 4-substituted 1,2,4-triazoline-3,5-diones, which is a multi-step reaction and requires a lot of time and effort [14].

We present here a new three-step route for modification of a styrene-butadiene copolymer, which consists of two polystyrene end blocks and a random styrene-butadiene middle block (S-S/B-S), via an epoxidation step with following hydrolysis of the epoxide [15], Steglich esterification [31] afterwards and finally a “Click” reaction step (copper catalyzed azide alkyne cycloaddition, CuAAC) which is regiospecific and leads to high yields [32, 33] (Figure 1). In 1909 Nikolaus Prileschajew reported the reaction of an alkene with a peroxy acid first [34]. The electrophilic oxygen atom of the meta-chloroperbenzoic acid (mCPBA) (which is given by the high polarization) is able to add to alkenes. Several mechanisms have been proposed but it is still not fully understood. Commonly accepted is the so called “Butterfly Mechanism” which is a concerted reaction with a transition state that resembles a butterfly [35, 36]. Steglich esterification is a possibility to conduct an esterification reaction under mild conditions which is also suitable for sterically demanding molecules like polymers. The carboxylic acid is activated by forming an *O*-acylisourea intermediate with dicarbodiimide (DCC) and can then be added to the alcohol. Dicyclohexylurea results as side product, which is insoluble in DCM and therefore DCM is often used as solvent. Due to the fact that the reaction of the *O*-acylisourea intermediate and an alcohol is slow and can lead to the formation of side products, 4-dimethylaminopyridine (DMAP) is used as a group transfer reagent which suppresses these side reactions [31, 37]. Copper catalyzed azide alkyne cycloaddition is a 1,3-dipolar cycloaddition reaction. An azide and terminal alkyne are forming a 1,2,3-triazole ring structure and the use of copper as catalyst leads to the 1,4-disubstituted regioisomer specifically [33].

The modification of (S-S/B-S) takes place statistically along the polymer chain on the butadiene units which are located in the middle block. In total this modification route includes well established reactions with high yields under mild conditions that are easy to perform and results in a toolbox of diverse functional block copolymers. Azide containing molecules with other functional groups can be synthesized separately and then are attached to the polymer easily by CuAAC. Especially for the introduction of

complex structures into the polymer (e.g. multiple hydrogen bonding motifs) this approach is attractive.

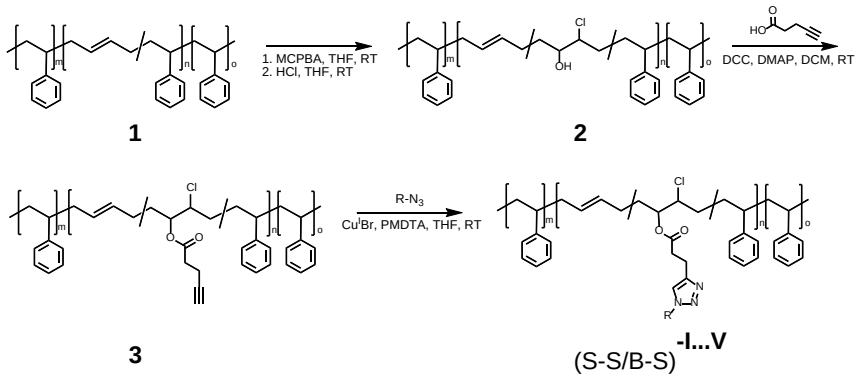

Figure 1: General reaction scheme for modification of S-S/B-S via three-step pathway.

Via this synthesis route we were able to obtain styrene-butadiene copolymers (S-S/B-S) with carboxylic acid functions along the polymer chain. Carboxylic acid functions pertain to bivalent hydrogen bonds and are one of the more simple interactions but can have a huge effect on the materials properties anyway [11]. A defined equilibrium between free and complexed species in the hydrogen bonding complex (Figure 2) can be observed and investigated by temperature-dependent infrared spectroscopy [38]. IR spectroscopy is a well suited tool for this purpose due to the well localized and intense vibrational mode of the carbonyl stretching. It allows the investigation of a particular region in the molecule and provides specific information about the vibrational transition. The effect of the vibrational transition can be directly monitored by IR spectroscopy. It is known that the associated C=O stretching vibration is found at lower frequencies than the unrestricted C=O stretching vibration because of the decrease in electron density of the carbonyl group due to the stretched C=O bond [39]. Therefore IR spectroscopy is an excellent tool to observe the complexation process. It is possible to clearly distinguish the free and complexed species by reason of the presence of an isosbestic point [40] and the application of Beer-Lambert law allows the quantitative analysis of the complex formation including the determination of enthalpy and entropy.
In this study we show the temperature dependency of complex formation monitored via FTIR spectroscopy. The modified polymer was therefore heated up and the carbonyl stretching vibration was quantitatively analyzed by peak integration. In the end we

found the equilibrium constant K of the observed system to be a function of temperature as well as the enthalpy and entropy of complex formation.

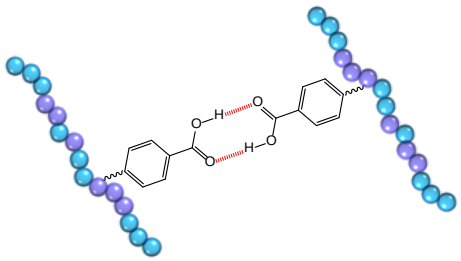

Figure 2: Dimerization of two carboxylic acid groups. The scheme shows two hydrogen bonding motifs which are interacting by forming a hydrogen bonding complex (indicated in red). Indicated in purple is polybutadiene which is partially modified along the chain and indicated in blue is polystyrene.

2. Experimental Section

2.1 Materials

Styroflex 2G66 is a triblock copolymer with styrene end blocks and a random styrene-butadiene middle block, with a number average molecular weight of M_n = 134000 g/mol, a polydispersity of PDI = 1.2 (M_n and PDI were determined via GPC with PS standards), a content of polybutadiene of 52.6 w% (determined by ^{1}H NMR) and was gratefully received from BASF, Germany. Copper(I) bromide (99.9%), meta-chloroperbenzoic acid (mCPBA, 77%), dicyclohexylcarbodiimide (DCC, 99%) and 4-dimethylaminopyridine (DMAP, 99%) were received from Sigma Aldrich, Germany. From Merck (Germany) ethyl bromoacetate (98%), hydrochloric acid (HCl, 37w%) as well as sodium azide (99%) were purchased. Acetone (99.8%), *n*-hexane (95%) and tetrahydrofurane (THF, 99.5%) were received from VWR, Germany. Dichlormethane (DCM, 99.9%) and 4-pentynoic acid (95%) were purchased from Acros Organics (Germany) while 4-azidobenzoic acid (97%) and N,N,N',N'',N''-pentamethyldiethylenetriamine (PMDTA, 98%) were received from TCI Chemicals, Belgium. Methanol (99%) was received from BCD Chemie (Germany) and sodium sulfate (99%) was purchased from Grüssing, Germany.

All experiments were done under inert conditions if not mentioned otherwise.

2.2 Epoxidation and Hydrolysis

The epoxidation and ring-opening reaction was performed according to the literature [15]. In a typical experiment 10.0 g (0.10 mol of C=C) of Styroflex 2G66 was weighed into a three-necked round-bottom flask equipped with dropping funnel and dissolved in 100 mL anhydrous THF in an inert atmosphere at room temperature. A solution of 3.00 g (17.4 mmol, 0.18 eq with respect to C=C) of mCPBA in 50 mL THF was added dropwise to the polymer solution and stirred overnight at room temperature. The resulting epoxide was turned into the targeted hydroxide via a ring-opening reaction by dropwise addition of 2.00 g (0.02 mol, 1.2 eq with respect to mCPBA) HCl in 20 mL THF over 1 hour at room temperature. The reaction solution was stirred for another 3 hours to complete the ring-opening reaction. The purification of the polymer was performed by three cycles of precipitation into 1500 mL methanol and redissolving the separated polymer in 200 mL THF. The purified polymer was dried under vacuum at 25°C overnight and was obtained as a colorless solid (10.29 g, 95% conversion, 92% yield).

2.2 Esterification

In a typical experiment 5.00 g (7.07 mmol of –OH) of the hydrochlorinated polymer, 1.40 g (14.3 mmol, 2 eq) 4-pentynoic acid and 9.28 mg (0.76 mmol, 0.1 eq) DMAP were dissolved in 70 mL anhydrous DCM. To this solution a solution of 2.95 g (14.3 mmol, 2 eq) DCC in 10 mL anhydrous DCM was added dropwise at room temperature. The reaction mixture was stirred overnight at room temperature. The purification of the polymer was performed (as mentioned before) by three cycles of precipitation into 800 mL methanol and redissolving the separated polymer in 70 mL DCM. The purified polymer was dried under vacuum at 25°C overnight and the product was obtained as a colorless solid (4.29 g, 84% conversion, 75% yield).

2.4 Preparation of azides

The preparation of the functional azides (**II-V**) from their bromide analogues was conducted as described in literature [41]. The synthesis of ethyl azidoacetate **II** is given here as an example. Therefore, 1.51 g (9.04 mmol) ethyl bromoacetate was dissolved in 10 mL of H_2O (2 mL) and acetone (8 mL). To this mixture 0.88 g (13.5 mmol, 1.5 eq) sodium azide was given and stirred overnight at ambient temperature. The purification was performed by extraction the reaction mixture three times with DCM, dried over

sodium sulfate and evaporating the solvent *in vacuo* to give the product as a colorless liquid (0.74 g, 5.73 mmol, 64% yield).

^{1}H NMR (400 MHz, $CDCl_3$): δ [ppm] = 4.26 (q, J = 7.2 Hz, 1H), 3.86 (s, 1H), 1.31 (t, J = 7.2 Hz, 2H).

^{13}C NMR (100 MHz, $CDCl_3$): δ [ppm] = 168.39, 76.91, 61.99, 50.54, 14.26.

2.5 Copper-catalyzed azide–alkyne cycloaddition

In a typical experiment [42] 1.00 g (1.20 mmol of alkyne groups) of the alkyne-modified polymer and 0.40 g (2.45 mmol, 2 eq) 4-azidobenzoic acid were dissolved in 40 mL anhydrous THF and degassed by three freeze-thawing cycles. After degassing, 35.0 mg (0.24 mmol, 0.2 eq) copper(I)bromide and 50 µL (0.24 mmol, 0.2 eq) PMDTA were added to the solution. The reaction mixture was stirred overnight at room temperature. An additional amount of 40 mL THF was given to the reaction solution and purified by aluminium oxide flash chromatography. The solution was concentrated *in vacuo* and the purification of the polymer was performed by three cycles of precipitation into 400 mL *n*-hexane and redissolving the separated polymer in 35 mL THF. The purified polymer was dried under vacuum at 25°C overnight and the product was obtained as a colorless solid (1.00 g, 94% conversion, 87% yield).

2.6 Characterization

NMR spectroscopic data were recorded on a Bruker Avance 400 MHz spectrometer using $CDCl_3$ as solvent with concentrations of about 15 g L^{-1}. All ^{1}H and ^{13}C NMR chemical shifts are quoted in ppm and the $CDCl_3$ signal at 7.26 ppm was used as an internal reference for the chemical shifts in ^{1}H NMR. The signals of the spectra containing modified and unmodified S-S/B-S polymers are normalized by unifying the integral of the aromatic styrene signal occurring in the range of 6.3 - 7.3 ppm.

Temperature-dependent FTIR spectra were recorded on a Bruker Vertex 70 in a range of 30 – 130°C with a resolution of 4 cm^{-1} and 50 scans per spectrum. The sample was heated to the chosen temperature and kept at this temperature for 15 minutes to achieve equilibrium. The samples for FTIR analysis were dissolved in DCM (5w% polymer solution) and casted on a KBr plate. The solvent was evaporated overnight at 30°C. A background measurement without a specimen in the sample compartment was conducted at ambient temperature and subtracted from the recorded data by the

Bruker software OPUS. Furthermore, there was no additional data processing applied to the recorded FTIR spectra.

DSC measurements were conducted on a DSC1 from Mettler Toledo. The experiments were run with a scanning rate of 5 K/min in a range of -150°C – 150°C and conducted in an inert nitrogen atmosphere maintain by a flow rate of 60 mL/min. Therefore, about 10 mg polymer was weighted into a 40 µL aluminium crucible which was closed afterwards. The data processing was performed by STARe Software, Version 12.10a.

3. Results and Discussion

3.1 Modification of styrene-butadiene based copolymers

The list of all modification reactions performed with styrene-butadiene based block copolymers (S-S/B-S) and azides **I-V** is provided in Table 1. The conducted reactions were monitored by ^{1}H NMR. An overview of the particular reaction steps for (S-S/B-S)-**I** are shown in Figure 3. As known from literature [15] the epoxidation of the polybutadiene using mCPBA is excellent in efficiency and easy to perform. The conversion rates are usually in the range of 95% to 100% and also the yields of the polymer after precipitation in methanol are almost quantitative (see Table 1). The conversion was calculated by using the integral ratios for the vinylic protons before and after the hydrochlorination using the styrene protons as reference. In the ^{1}H NMR spectra of the hydrochlorinated polymer (Figure 3, spectrum ii) two additional signals (peaks a and b) can be observed which are attributed to the methine protons in the polymer backbone next to the functional groups. The esterification step via Steglich esterification also provides high conversion rates in the range of 84 to 100%. They are calculated by using the integral ratios of the methine protons linked to the hydroxyl group before and after the Steglich esterification by taking the styrene protons as a reference again. The precipitation in methanol gives yields of about 54% to 82% of the esterificated polymer. In the ^{1}H NMR spectra of the esterified polymer (Figure 3, spectrum iii) the signal for the methine proton (next to the secondary hydroxyl group) in the backbone is shifted further down-field from δ = 3.70 ppm (peak a) to δ = 5.10 ppm (peak e). This observation is in good agreement with values found in literature [43] and indicates the successful grafting of the 4-pentynoic acid linker. Two additional overlapping signals at δ = 2.54 ppm and δ = 2.59 ppm appear which can be attributed to the two methylene groups in the linker molecule (peaks c and d). The CuAAC reaction is also well known from literature [33], easy to handle and give almost

quantitative conversion rates also for modification of polymers although the reactivity in polymers is often decreased in contrast to low molecular weight molecules. Therefore, the preparation of the azides which shall be introduced into the polymer is necessary. The synthesis of the azides from their bromide analogues is well known and often described [41, 44, 45]. The success of the reaction is hard to analyze by ^{1}H NMR, because the chemical shift for the protons next to the bromide or azide is quite similar. A very useful characterization method for the azide is the ^{13}C NMR spectroscopy. The chemical shift for the carbon atom next to the azide is much more shifted down-field compared to the bromide analogue and helps in that way to monitor the reaction. In case of the azide **II** it is δ = 50.54 ppm for the carbon atom next to the azide group and δ = 25.9 ppm [46] for the analogue bromide.

The conversion rates achieved for the CuAAC reaction are in a range of 83% to 93%. They are determined by using the integral ratios of the methylene protons attributed to the linker before and after the click reaction step at δ = 2.54 ppm and δ = 2.59 ppm taking the styrene protons as reference again. After the completed CuAAC reaction (Figure 3, spectrum iv) the signals for the methylene group protons are split up and shifted further down-field from δ = 2.54 ppm (peak c) and δ = 2.59 ppm (peak d) to δ = 2.87 ppm (peak f) and δ = 3.16 ppm (peak g). Another proof of success is indicated by the signal occurring at δ = 7.95 ppm (peak h). The signal is attributed to the proton of the triazole ring [47] which forms during the reaction. With this we can be sure that the reaction succeeded well.

The presented reaction pathway offers a broad variety of post modification. Following these steps it is possible to introduce almost arbitrary azides into the polymer to obtain functional polymers. Some functional azides (**II-V**) were already prepared as given in the experimental section and successfully used to modify the S-S/B-S polymer (Figure 4, Supplementary Information). The modification reactions result in carboxylic acid, ester, hydroxyl and nitrile functional groups, respectively. So this approach allows the introduction of functional groups into the polymer along the chain in a manifold manner and gives new opportunities for modification strategies resulting in a kind of toolbox.

Table 1: List of modification reactions performed with a styrene-butadiene based block copolymer (S-S/B-S) and azides **I-V** (Figure 4). For each reaction step (epoxidation/hydrolysis, Steglich esterification and CuAAC) conversion rate and yield (determined by ^{1}H NMR) of the reaction is given as well as the overall degree of modification D_m.

Sample	**Epoxidation/ Hydrolysis**		**Steglich esterification**		**CuAAC**		***D*$_m$[1]**
	Conversion [%]	Yield [%]	Conversion [%]	Yield [%]	Conversion [%]	Yield [%]	[%]
(S-S/B-S)-**I**	95	92	84	75	94	87	6
(S-S/B-S)-**II**	100	97	100	59	91	44	8
(S-S/B-S)-**III**	100	97	98	54	93	75	8
(S-S/B-S)-**IV**	95	92	84	75	93	79	6
(S-S/B-S)-**V**	95	92	84	75	91	85	6

[1] The overall degree of modification was calculated from ^{1}H NMR spectra after hydrochlorination reaction as well as multiplication with the conversion rates of the subsequent reaction steps and is given by $D_m = (1- (\int PB_{after} / \int PB_{before})) \cdot c_S \cdot c_C$. The decrease of the polybutadiene signal (PB) after the hydrochlorination was used to calculate the degree of modification. Multiplication with the conversion rates (c_s and c_c)

of the subsequent reaction steps results in the overall degree of modification.

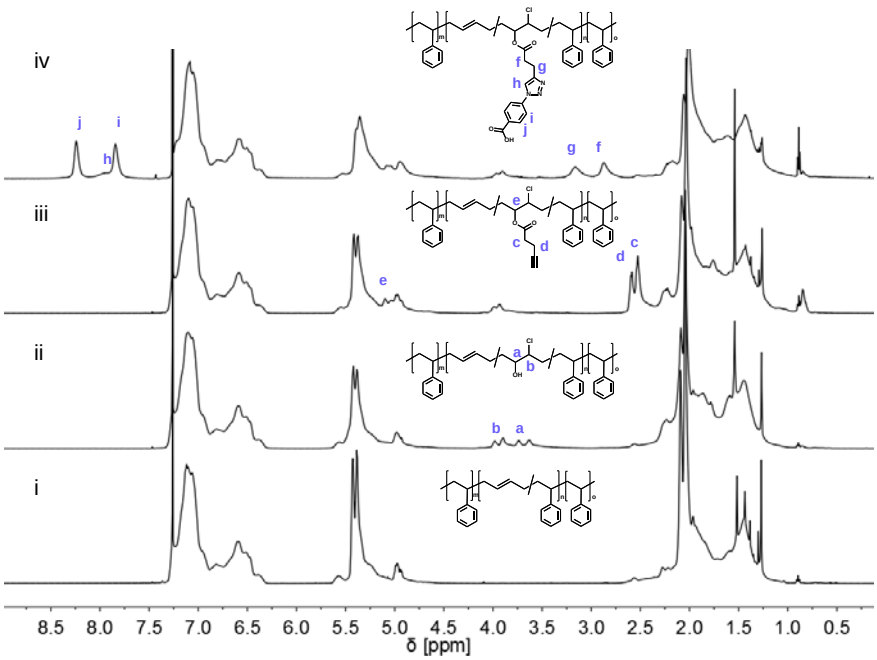

Figure 3: ^{1}H NMR spectra of modified (S-S/B-S)-**I**. According to the presented modification route the spectra are given from bottom to top: i) S-S/B-S, ii) (S-S/B-S)-**OH**, iii) (S-S/B-S)-**C≡C** and iv) (S-S/B-S)-**I**.

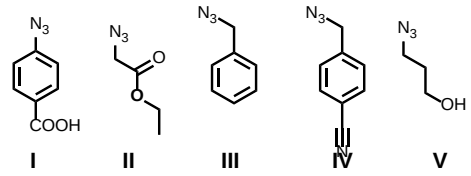

Figure 4: Chemical structure of the azides used for CuAAC reaction: I) 4-azidobenzoic acid, II) ethyl azidoacetate, III) benzyl azide, IV) 4-(azidomethyl)benzonitrile, V) 3-azido-1-propanol.

3.2. Temperature dependent IR spectroscopy

The polymer (S-S/B-S)-**I** contains a hydrogen bonding motif with carboxylic acids along the polymer chain. These carboxylic acids can interact with each other and form

hydrogen bonding complexes. The complex formation can spectroscopically be characterized by temperature dependent IR spectroscopy analyzing the C=O stretching vibration. The temperature dependent IR spectra were conducted in a range of 30°C – 130°C (Figure 5). In the region of the carbonyl stretching vibration three signals at the positions 1738 cm^{-1}, 1700 cm^{-1} and 1685 cm^{-1} can be distinguished. The signal at 1738 cm^{-1} is attributed to the free carbonyl stretching vibration while the associated stretching vibration can be observed at 1700 cm^{-1} as well as at 1685 cm^{-1}. This indicates the presence of at least two types of associated species. The carbonyl stretching vibration at 1700 cm^{-1} can be assigned to the dimeric complex [38] while the signal at 1685 cm^{-1} is attributed to more complex superstructures. The integral ratios of these three signals for the carbonyl stretching vibration are changing with temperature. With the increase of temperature the signal intensity for the free carbonyl stretching vibration increases and that of the complexed carbonyl stretching vibration decreases. This is due to the fact that the hydrogen bonding complexes are less stable at higher temperatures. At ambient temperature the integral areas for the free species (A_f) are much lower in comparison to the complexed species (A_a), but the higher becomes the temperature the hydrogen bonds of the associated species are dissociating. This leads to increased integral areas A_f and decreased integral areas A_a (Figure 6a). At 1707 cm^{-1} the total absorbance of the sample is equal during the heating cycle which results in the observation of a crossing point of all spectra – the isosbestic point [40]. The presence of the isosbestic point indicates in general a defined equilibrium between two states and the validity of Beer-Lambert law [38]. In our case it is the defined equilibrium between the free carboxylic acid and the associated one (equation 1) with the equilibrium constant K (equation 2).

$$C{=}O_{free} \rightleftharpoons C{=}O_{associated} \quad (1)$$

$$K = \frac{[C{=}O]_{associated}}{[C{=}O]_{free}} \quad (2)$$

From Luckhaus et al. [48] we know that the eight-ring model of carboxylic acid dimers should be replaced by a new understanding of this complex by a so-called “monomers-in-dimers” model. They found the coupling mechanisms to be the same for the monomer and the dimer and also the short time dynamics are dominated by the monomers. This leads to the conclusion that the carboxylic acid dimer should be more seen as two monomers than an eight-ring complex. Also the bond distances in the

dimer support this conclusion. The C=O bond length in an acetic acid dimer is calculated and found to be 1.211 ± 0.004 Å [48-50] for the monomer and for the dimer it is about 1.230 ± 0.003 Å [48-50]. The bond length is enlarged but still very close to the length found in the monomer. This becomes even more obvious when we have a look on the bond length of the hydrogen bond O-H···O which is about 2.698 ± 0.031 Å [48, 50].

From this we conclude the equilibrium to be formulated as seen above: we focus on one carboxylic acid group which is free in one state and bound in another. It is noteworthy that the carbonyl stretching vibration of the ester group bound directly at the polymer backbone occurs in the same region. The integral area of the carbonyl stretching vibration of the ester group was subtracted from the original data.

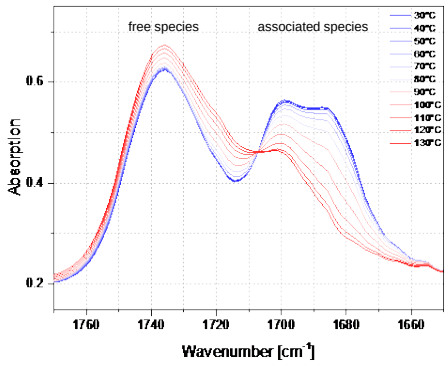

Figure 5: Temperature-dependent IR spectra (1650 cm^{-1} – 1770 cm^{-1}) in the range of 30°C-130°C show a clear crossing point for all spectra (isosbestic point) at 1707 cm^{-1}; absorption spectra as measured.

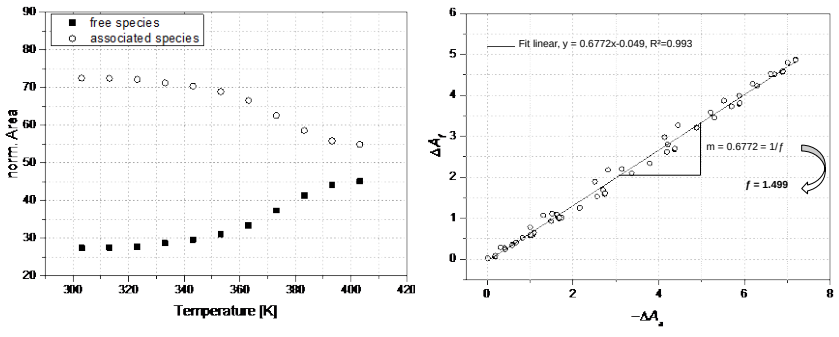

Figure 6: a) Integrated and normalized IR peak area after subtraction of the integral area of the ester group is plotted as a function of temperature. The filled squares show the increase of integral peak area with temperature for the free species while the open

circles show the decrease of integral peak area with temperature for the associated species. b) The increase of the peak area of the free species, ΔA_f as a function of the decrease of the peak area of the associated species, $-\Delta A_a$ results in a straight line giving the ratio of extinction coefficients f.

The validity of Beer-Lambert law is proven by the presence of the isosbestic point and allows the quantitative analysis of the temperature dependent IR measurements. This gives a more detailed insight into the thermodynamics of this system by calculating the enthalpy and entropy of complex formation. Applying Beer-Lambert law and plotting the increase of the area for the free carboxylic acid ΔA_f as a function of the decrease of the area for the associated carboxylic acid $-\Delta A_a$ for any temperature difference gives the ratio of extinction coefficients [38, 51] (equation 3, Figure 6b).

$$\frac{-\Delta A_a}{\Delta A_f} = \frac{\varepsilon_a}{\varepsilon_f} = f \qquad (3)$$

A linear regression represents the data points best and the slope of it is determined to be $m = 0.6772$ and its reciprocal value gives the ratio of extinction coefficients ($f = 1.499$). With knowledge of the ratio of extinction coefficients the equilibrium constant K (equation 2) for the already expressed equilibrium can be determined by calculating the mole fractions of the free and associated carboxylic acids first (equation 4).

$$x_a = \frac{A_a}{A_f \cdot f} \cdot \frac{1}{\left(1+\frac{A_a}{A_f \cdot f}\right)} \qquad (4)$$

With this knowledge the equilibrium constant K for each measured temperature is accessible and therefore the vant 't Hoff plot where ln K is plotted as a function of 1/T can be applied. In Table 2 the integrated areas of the signals, the mole fractions of the free and associated carboxylic acids are given as well as the values calculated for ln K. In Figure 7 is shown the vant 't Hoff plot obtained from this data set.

Table 2: Temperature dependence of integrated and normalized peak areas (in percent), mole fractions for associated and free carboxylic acid groups and ln K.

T [°C]	area [%]	A_a [%]	A_f [%]	x_a	x_f	ln K
30	100.00	72.49	27.51	0.64	0.36	0.56
40	100.03	72.44	27.56	0.64	0.36	0.56
50	99.67	72.17	27.83	0.63	0.37	0.55
60	99.32	71.23	28.77	0.62	0.38	0.50
70	98.78	70.35	29.65	0.61	0.39	0.46
80	98.01	68.87	31.13	0.60	0.40	0.39
90	96.61	66.57	33.43	0.57	0.43	0.28
100	95.00	62.60	37.40	0.53	0.47	0.11
110	93.82	58.61	41.39	0.49	0.51	-0.06
120	93.16	55.83	44.17	0.46	0.54	-0.17
130	93.10	54.87	45.13	0.45	0.55	-0.21

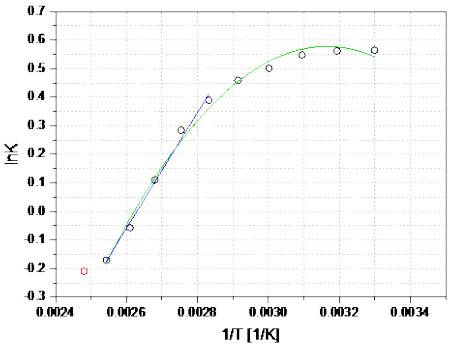

Figure 7: Van 't Hoff plot is obtained by plotting ln K as a function of 1/T. The straight blue line shows the temperature region (80°C – 130°C) in which a linear dependence of ln K and 1/T is observed. The regression equation for the blue line is ln K = 2027.3 1/T – 5.33 with $R^2 = 0.996$. The green curve shows the fit curve which represents all data points well and is observed by applying a polynomial fit. The regression equation for the blue line is ln K = 12407.2 T^{-1} – 1.96 · 10^{-6} $1/T^2$ – 19.1 with $R^2 = 0.990$. In red indicated is a data point which is not taken into consideration.

From Figure 7 it can be seen that there is a nonlinear relationship between ln K and 1/T. Only for elevated temperatures in a range from 80°C to 130°C a linear van 't Hoff plot is observed (blue line). In this region it is acceptable to apply the vant 't Hoff

equation to determine enthalpy of complex formation from the slope of the line and entropy of complex formation from the intercept. But in the temperature range below 80°C there is a deviation from the linear behavior. The linear behavior is based on the assumption that enthalpy and entropy are independent from temperature. This is not the case for the system presented here. There is an obvious change of ln K with temperature and thus with enthalpy and entropy of complex formation as well. This was also observed by other groups [38, 52]. Well known and more often observed is this phenomenon in chromatographical studies [53-55]. As explanation is given the structural modification and therefore a change in heat capacity of the two examined species during formation and cleavage of the complex [54]. This is a reasonable explanation if one thinks of the structural change during disruption of the supramolecular structure. By DSC measurements (Figure 8) we found in addition to the shift of the glass transition temperature from -54°C for unmodified S-S/B-S to 59°C for (S-S/B-S)-**I** a clear endotherm transition beginning at 75 – 80°C which should be related to the opening of the hydrogen bond complex and therefore the collapse of the supramolecular structure. Also Hilger et al. [29] found besides the glass transition of the polymer a second endotherm transition at 80°C for a benzoic acid modified polybutadiene. This system is comparable with the one shown here and supports the explanation of a structural modification.

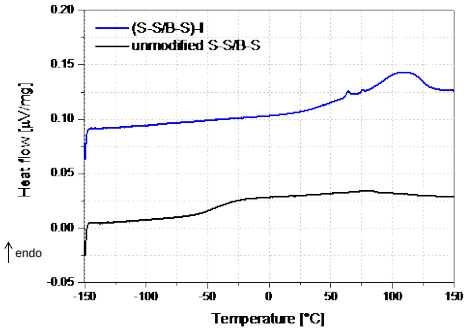

Figure 8: DSC measurements of unmodified S-S/B-S and (S-S/B-S)-**I** in the temperature range of -150 – 150°C are presented. In black shown is the unmodified S-S/B-S and shown in blue is (S-S/B-S)-**I** to which 0.05 µV/mg was added for better clarity. The third heating rates are shown.

Taking this into account a second term in vant 't Hoff equation appears which considers the equilibrium constant to be a function of temperature and results in an extended

expression for the vant 't Hoff equation [54] (equation 5) and finally in a more accurate fit line representing the data set accurately (green line).

$$\ln K = \alpha_0 + \frac{\alpha_1}{T} + \frac{\alpha_2}{T^2} \quad (5)$$

Thus, enthalpy and entropy as functions of temperature can be calculated (equation 6 and 7).

$$\Delta H = -R \left(\alpha_1 + 2 \frac{\alpha_2}{T} \right) \quad (6)$$

$$\Delta S = -R \left(\alpha_0 - \frac{\alpha_2}{T^2} \right) \quad (7)$$

At elevated temperatures the enthalpy of complex formation is determined to be ΔH = -16.9 kJ/mol and the entropy of complex formation is determined to be ΔS = -44.3 J/(mol K) by application of the linear vant 't Hoff equation. Using the extended vant 't Hoff equation the ΔH and ΔS can be determined as function of temperature. Some values are listed in Table 3. The values determined for complex formation are consistent with the physical chemistry of complex formation. The change in enthalpy is negative which means that the formation of the hydrogen bond complex is enthalpically favored. In other words the break of the hydrogen bond requires energy from the system. Accordingly, the formation of the hydrogen bond gives stabilization energy to the system. The change in entropy of complex formation is negative as well. This shows, that the complex formation means loss in entropy in the system which is also quite intuitive. This disorder in the system decreases or the order in the system increases when hydrogen bond complexes are formed. Besides local ordering also the conformational entropy of the polymer chains is reduced. The values of enthalpy obtained for complex formation are slightly lower than obtained for urazole modified squalene [38] or poly(vinylphenol) blended with ethylene-vinylacetate [52]. The enthalpy of complex formation was determined to be -28.6 kJ/mol for the urazole modified squalene and -21.3 kJ/mol for the or poly(vinylphenol) blended with ethylene-vinylacetate. In both cases the complex formation of at least one low molecular weight compound is investigated and therefore the comparability is poor. Also not taken into account is the possibility that only one hydrogen bond might be formed between two of the benzoic acid units. A decreased value for the enthalpy could support the idea of having not only bivalent complexation. The value for the entropy fits quite good to the reported values [38].

Table 3: Thermodynamic data of hydrogen bond complex formation.

T [°C]	ΔH [kJ/mol]	ΔS [J/(mol K)]
30	4.35	18.94
40	0.92	7.79
50	-2.30	-2.33
60	-5.33	-11.56
70	-8.18	-19.99
80	-10.87	-27.72
90	-13.41	-34.82
100	-15.81	-41.35
110	-18.09	-47.38
120	-20.26	-52.96
130	-22.31	-58.12

4. Conclusion

The implementation of a new and simple modification route for styrene-butadiene copolymers was accomplished which should also be applicable to polydienes or diene containing copolymers. Using a reaction pathway including an epoxidation with subsequent hydrolysis step and Steglich esterification as well as CuAAC reaction afterwards leads to a toolbox of diverse functional block copolymers which are modified statistically along the polymer chain. All reactions performed give high yields and are easy to conduct. Therefore this modification route is a powerful way to “click” functional groups into styrene-butadiene copolymers. The functional groups can be synthesized and prepared separately which makes this approach attractive especially for the introduction of more complex functional motifs. Along this pathway we obtained an S-S/B-S triblock copolymer which is statistically modified with carboxylic acid functional groups along the polymer chain. These carboxylic acid functions are undergoing a dimerization process at ambient temperatures by forming hydrogen bonds. They are breaking apart at elevated temperatures. This was investigated via temperature-dependent IR spectroscopy. We found the equilibrium constant of the monomer-dimer equilibrium to be a function of temperature as well as the thermodynamic parameters ΔH *and* ΔS*.*

Acknowledgement

The authors thank Silvio Neumann (Helmholtz-Zentrum Geesthacht) for performing the DSC experiments and Md. Mushfequr Rahman for helpful discussions. We gratefully acknowledge financial support from the German Research Foundation (DFG) via SFB986 "M^3", project A2.

References

1. Burattini S, Greenland BWG, Merino DHM, Weng WW, Seppala J, Colquhoun HM, Hayes W, Mackay ME, Hamley IW, and Rowan SJ. Journal of American Chemical Society 2010;132(34):12051-12058.
2. Burnworth M, Tang L, Kumpfer JR, Duncan AJ, Beyer FL, Fiore GL, Rowan SJ, and Weder C. Nature 2011;472(7343):334-337.
3. Sijbesma RP, Beijer FH, Brunsveld L, Folmer BJB, Hirschberg JHKK, Lange RFM, Lowe JKL, and Meijer EW. Science 1997;278:1601-1604.
4. Cordier P, Tournilhac F, Soulie-Ziakovic C, and Leibler L. Nature 2008;451(7181):977-980.
5. Yan T, Schröter K, Herbst F, Binder WH, and Thurn-Albrecht T. Macromolecules 2014;47(6):2122-2130.
6. Yan T, Schroter K, Herbst F, Binder WH, and Thurn-Albrecht T. Sci Rep 2016;6:32356.
7. Herbst F, Dohler D, Michael P, and Binder WH. Macromol Rapid Commun 2013;34(3):203-220.
8. Aida T, Meijer EW, and Stupp SI. Science 2012;335:813-817.
9. Mes T, Koenigs MME, Scalfani VF, Bailey TS, Meijer EW, and Palmans ARA. ACS Macro Letters 2012;1(1):105-109.
10. Seidel U, Hellman J, Schollmeyer D, Hilger C, and Stadler R. Supramolecular Science 1995;2:45-50.
11. Binder W and Zirbs R. Hydrogen Bonded Polymers. Heidelberg: Springer-Verlag, 2007.
12. Hellmann J, Hilger C, and Stadler R. Polymers for Advanced Technologies 1994;5:763-774.
13. R.Stadler. Macromolecules 1988;21(1):121-126.
14. Billiet S, De Bruycker K, Driessen F, Goossens H, Van Speybroeck V, Winne JM, and Du Prez FE. Nat Chem 2014;6(9):815-821.
15. Peng C-C and Abetz V. Macromolecules 2005;38:5575-5580.
16. Stadler R and Freitas LdL. Colloid & Polymer Science 1986;264:773-778.
17. van der Heijden S, De Bruycker K, Simal R, Du Prez F, and De Clerck K. Macromolecules 2015;48(18):6474-6481.
18. Ribeiro S, Costa P, Ribeiro C, Sencadas V, Botelho G, and Lanceros-Méndez S. Composites Part B: Engineering 2014;67:30-38.
19. Wu L, Ma H, Wang Q, Li L, Wang Y, and Li Y. Journal of Materials Science 2014;49(14):5171-5181.
20. Albuerne J, Fierro AB-d, Abetz C, Fierro D, and Abetz V. Advanced Engineering Materials 2011;13(8):803-810.
21. Chernyy S, Ullah S, Jomaas G, Leisted RR, Mindykowski PA, Ravnsbæk JB, Tordrup SW, and Almdal K. European Polymer Journal 2015;70:136-146.
22. Dewar MJS and Fahey RC. Journal of the American Chemical Society 1963;85(15):2245-2248.

23. Bernasconi CF. Tetrahedron 1989;45(13):4017-4090.
24. Hoyle CE and Bowman CN. Angew Chem Int Ed Engl 2010;49(9):1540-1573.
25. Justynska J, Hordyjewicz Z, and Schlaad H. Polymer 2005;46(26):12057-12064.
26. Stadler R, Jacobi MM, and Gronski W. Makromol. Chem., Rapid Commun 1983;4:129-135.
27. Rout SR and Butler GB. Polymer Bulletin 1980;2:513-520.
28. Butler GB and Williams AG. Journal of Polymer Science 1979;17:1117-1128.
29. Hilger C and Stadler R. Makromol. Chem. 1990;191:1347-1361.
30. Hilger C and Stadler R. Makromol. Chem. 1991;192(4):805-817.
31. Neises B and Steglich W. Angew Chem Int Ed Engl 1978;17(7):522-523.
32. Sun S and Wu P. J. Phys. Chem. 2010;114:8331–8336.
33. Haldon E, Nicasio MC, and Perez PJ. Org Biomol Chem 2015;13(37):9528-9550.
34. Prileschajew N. Berichte der deutschen chemischen Gesellschaft 1909;42(4):4811-4815.
35. Dryuk VG. Tetrahedron 1976;32:2855-2866.
36. Kim C, Traylor TG, and Perrin CL. J Am Chem Soc 1998;120:9513-9516.
37. Neises B and Steglich W. Organic Syntheses 1985;63:183.
38. Freitas LdL, Auschra C, Abetz V, and Stadler R. Colloid Polymer Science 1991;259:566-575.
39. Guerin AC, Riley K, Rupnik K, and Kuroda DG. Journal of Chemical Education 2016;93(6):1124-1129.
40. Schlafer HL and Kling O. Angewandte Chemie 1956;68:667-670.
41. Berry MT, Castrejon D, and Hein JE. Org Lett 2014;16(14):3676-3679.
42. Lutz J-F, Börner HG, and Weichenhan K. Macromol Rapid Commun 2005;26(7):514-518.
43. Chen M, Li M, Wang H, Qu S, Zhao X, Xie L, and Yang S. Polym. Chem. 2013;4(3):550-557.
44. Bevilacqua V, King M, Chaumontet M, Nothisen M, Gabillet S, Buisson D, Puente C, Wagner A, and Taran F. Angew Chem Int Ed Engl 2014;53(23):5872-5876.
45. Gann AW, Amoroso JW, Einck VJ, Rice WP, Chambers JJ, and Schnarr NA. Org Lett 2014;16(7):2003-2005.
46. Alvarez-Sanchez R, Basketter D, Pease C, and Lepoittevin J-P. Chemical Research in Toxicology 2003;16(5):627-636.
47. Stadermann J, Riedel M, and Voit B. Macromolecular Chemistry and Physics 2013;214(2):263-271.
48. Emmeluth C, Suhm MA, and Luckhaus D. The Journal of Chemical Physics 2003;118(5):2242-2255.
49. van Eijck BP, Opheusden J, van Schaik MMM, and van Zoeren E. Journal of Molecular Spectroscopy 1981;86:465-479.
50. Derissen JL. Journal of Mofecular Structure 1970;7:67-80.
51. Stadler R and Freitas LdL. Polymer Bulletin 1986;15:173-179.
52. Moskala EJ, Howe SE, Painter PC, and Coleman MM. Macromolecules 1984;17:1671-1678.
53. Cunliffe JM, Dreyer DP, Hayes RN, Clement RP, and Shen JX. J Pharm Biomed Anal 2011;54(1):179-185.
54. Galaon T and David V. J Sep Sci 2011;34(12):1423-1428.
55. Guo H-X, Wu S, and Sun J. Molecules 2013;19(1):9-21.

1